

Southern Illinois University Carbondale

OpenSIUC

---

Research Papers

Graduate School

---

Spring 4-8-2022

## TRIAXIAL FORCE SENSOR CONFIGURARATION OF AN IN-GROUND FORCE PLATFORM

Kailey Reynolds  
kailey.reynolds@siu.edu

Follow this and additional works at: [https://opensiuc.lib.siu.edu/gs\\_rp](https://opensiuc.lib.siu.edu/gs_rp)

---

### Recommended Citation

Reynolds, Kailey. "TRIAXIAL FORCE SENSOR CONFIGURARATION OF AN IN-GROUND FORCE PLATFORM." (Spring 2022).

This Article is brought to you for free and open access by the Graduate School at OpenSIUC. It has been accepted for inclusion in Research Papers by an authorized administrator of OpenSIUC. For more information, please contact [opensiuc@lib.siu.edu](mailto:opensiuc@lib.siu.edu).

TRIAXIAL FORCE SENSOR CONFIGURARATION OF AN IN-GROUND FORCE  
PLATFORM

by

Kailey Reynolds

B.S., University of Wisconsin-Whitewater, 2020

A Research Paper

Submitted in Partial Fulfillment of the Requirements for the  
Master of Science in Education

School of Human Sciences  
in the Graduate School  
Southern Illinois University Carbondale  
May 2022

RESEARCH PAPER APPROVAL

TRIAXIAL FORCE SENSOR CONFIGURATION OF AN IN-GROUND FORCE PLATFORM

By

Kailey Reynolds

A Research Paper Submitted in Partial  
Fulfillment of the Requirements  
for the Degree of  
Master of Science in Education  
in the field of Kinesiology

Approved by:  
Sean Quisenberry, PhD, Chair

Graduate School  
Southern Illinois University Carbondale  
April 1, 2022

## TABLE OF CONTENTS

<u>CHAPTER</u>	<u>PAGE</u>
LIST OF TABLES .....	ii
LIST OF FIGURES .....	iii
CHAPTERS	
CHAPTER 1– Introduction.....	1
CHAPTER 2 – Methodology.....	4
CHAPTER 3– Results.....	8
CHAPTER 4 – Discussion.....	10
REFERENCES .....	12
VITA .....	14

## LIST OF TABLES

<u>TABLE</u>	<u>PAGE</u>
Table 1 – Three-by-three diagonal sensitivity matrix produced for the designed sensor .....	8
Table 2 -Measurement error and cross talk reading of the sensor .....	8

## LIST OF FIGURES

<u>FIGURE</u>	<u>PAGE</u>
Figure 1 – Triaxial loading cell with strain-gauge placement (top).....	6
Figure 2 – Triaxial loading cell with strain-gauge placement (side) .....	7
Figure 3 – Strain-gauge alignment/marketing tool.....	7
Figure 4 – Calibration Linearity of the Z Axis with Y Axis Crosstalk.....	9

## CHAPTER 1

### INTRODUCTION

Newton's third law states that when two bodies interact, they apply forces to one another that are equal in magnitude and opposite in direction. This principle can be quantified using force transducers, but in the realm of human movement, one of the most common instruments to quantify these reaction forces is a force platform or force plate (FP). Comprised of an arrangement of sensors allowing researchers and clinicians to compute ground reaction force (GRF), the force exerted on the body with equal and opposite direction and magnitude.

Historically, the pairing of GRF and lower extremity kinematics has become a vital tool for understanding lower extremity injury mechanisms, given researchers and clinicians to have the ability to compute segment and joint kinetics via inverse dynamics (Bruening & Takahashi, 2018). Inverse dynamics is the process of using kinematic data paired with force location (center of pressure, cop), direction, and magnitude of forces exerted on the segment of interest. Resulting in the computation of joint moments, contract forces, and loading during various forms of locomotion. Helping clinicians make inferences about GRF and center of mass to better understand risk factors associated with anterior cruciate ligament (ACL) injuries (Bates, Ford, Myer, & Hewett, 2013).

Recently, in-ground and portable FP have become a tool for athletic development. Used to assess athlete progress and training protocol effectiveness (Baker, Wilson, & Carlyon, 1994). More specifically, tracking the development of lower extremity explosive strength, a predictor of improved athletic characteristics such as sprinting (Weyand, Sternlight, Bellizzi, & Wright, 2000), jumping (Cormie, McGuigan, & Newton, 2010), and throwing velocity (Baena-Raya et al., 2021). This monitoring of athletic progress is achieved by examining the vertical force

impulse-momentum relationship during the take-off phase of various jumping techniques (Conceição, Lewis, Lopes, & Fonseca, 2022; Naves, Pereira, Andrade, & Soares, 2009).

Force plates are commonly comprised of superior and inferior aluminum or steel plates encompassing a variety of sensor arrangements. The first and most traditional sensor arrangements utilize four triaxial force sensors located at the outer four corners of a square or rectangular configuration. The force sensors are positioned at equal distances from an origin located at the center of the FP configuration. Each of the twelve forces are used to calculate six fundamental parameters (three force and three moments) utilized as part of inverse dynamics computations. The three axial forces quantify vertical force magnitude (Vertical, Z-axis), anterior-posterior force magnitude (AP, Y-axis), and medio-lateral force magnitude (ML, X-axis) in the global coordinate system; the three moments are computed using origin coordinate offsets and corresponding force measurements. The moments about the AP ( $M_y$ ) and ML ( $M_x$ ) axis use vertical force components to quantify plate moments, and the moment about the vertical axis ( $M_z$ ) is computed using shear force measurements. The  $M_y$  and  $M_x$  moments are used to quantify the location of force application, commonly referred to as the center of pressure. The second configuration utilizes a single podium multi-axis design that directly measures the aforementioned six force and moment components.

Force sensors frequently use strain gauges to quantify static and dynamic material deformation as a result of the compressive and tensile loading of the material (Lin, Ahmad, & Kebede, 2020). As the material deforms, the bonded strain gauge will elongate (tensile) or compress (compression), resulting in a change in electrical resistance during load application. Due to the rigidity of the FP, sensor deformation is limited to prevent notable surface motion



during load application resulting in required electrical signal amplification ranging from 100-10,000x.

In 1981, a short communication by Norman C. Heglund (1981) presented ideal force-plate characteristics for high precision GRF measurements and are as follows:

1. Be able to resolve the vertical, forward, and lateral components of the force
2. Have low 'crosstalk' between the measured components of the force
3. Have sufficient sensitivity and resolution for the subject of interest
4. Have a linear response
5. Have a response independent of where on the plate surface the force is exerted
6. Have a high natural frequency of oscillation
7. Have sufficient safety margin to protect both the plate and the subject from damage due to failure
8. Be simple and inexpensive

In order to achieve all eight characteristics, the traditional four triaxial force sensor configuration should be developed due to its ability to minimize mechanical crosstalk by independently quantifying FP force and moments. Unlike the single podium multi-axis force/moment sensors, the ability to reject mechanical crosstalk is limited to sensor design (Kebede, Ahmad, Lee, & Lin, 2019; Lin et al., 2020). Therefore, the object of this project was to determine the validity and reliability of a custom triaxial force sensor for use in the development of custom force plates.

## CHAPTER 2

### METHODOLOGY

This section presents the structural design and strain gauge arrangement for a triaxial force sensor that will be utilized to obtain the desired output of the force components of an in-ground force platform. Figure 1 illustrates the developed design of the triaxial force sensor utilizing a Maltese cross-element configuration to improve force measurement and reduce crosstalk. An aluminum alloy (7075-T6) was selected for fabricating the sensor.

#### Strain Gauge Arrangement

This study used 16 strain gauges from Omega (SGD-3/350-XY43) with resistance of  $350\ \Omega$  was used as a transducer. Each set of four strain gauges were arranged into three full Wheatstone bridge circuit, with each cross-element of the sensor utilized a half Wheatstone bridge configuration to quantify bending strain and rejecting compression strain. The combined half-bridge design resulted in two bridge resistances  $700\ \Omega$  for the Z axis and  $350\ \Omega$  of the X and Y axes, respectively.

An alignment tool was 3D printed (Hongkong Anycubic Technology Co., Limited, Kowloon, Hong Kong) to optimize strain gauge positioning at the location of maximum deformation for optimal sensitivity along the applied force axes (Figure 3). This tool was removed, a strain gauge was bonded to the surface using factory installation recommendations for 7075 aluminum alloy. The surface was wet and dry abraded using 320 grit and 400 grit wet/dry silicon carbide sandpaper, then surface pH was neutralized to improve adhesive bond using a diluted hyaluronan solution. Strain gauges were bonded to the surface using a cold-curing strain-gage adhesive (Loctite Model 496, Loctite® Brand, Westlake, Ohio).

## Calibration Setup

The calibration procedure of the sensor was performed to determine triaxial calibration/compensation matrix. Triaxial sensors have the highest levels of crosstalk between Z and X/Y components. Therefore, an accurate calibration process is required.

The calibration setup allowed each axis of interest/calibration axis to be orientated perpendicular to reference force under gravitational pull. Prior to each measurement sensor orientation was confirmed using a dual X/Y axis digital protractor (, DXL360S) and traditional bubble level. See Figure 4.

The calibration procedure is as follows:

1. Zero Point of the output signal of the three unfiltered channels.
2. Forces are applied to the mounted triaxial force sensor through hanging weights sixteen weights ranging from 19N to 710N.
3. Five trial of five seconds were collected for each axis.

## Data Acquisition and Processing

Signals were acquired using a 24-bit analog to digital data acquisition board (Model USB-1818, Measurement Computing Corp, Norton, Massachusetts) and recorded on a laptop computer. A custom program was written in LabVIEW (Version 2019, National Instruments, Austin, Texas) for data collection. Data were collected for 5 seconds at 50 Hz then saved to a comma separated values (.csv) with naming nomenclature corresponding to the calibrated axis, applied load, and trail number (Axis\_Force\_Trial, example AZ\_F0000\_T#). Files were then imported into MATLAB (version R2019b, MathWorks Inc., Natick, MA, USA) for data processing and analysis. Data for each channel was filtered using a zero-phase shift 4-pole Butterworth lowpass filter with a cutoff frequency of 10Hz. To account for signal

abnormalities resulting from signal filtering, the first and last 50 samples were discarded, and a mean value for each electrical signal was computed (points 50-150).

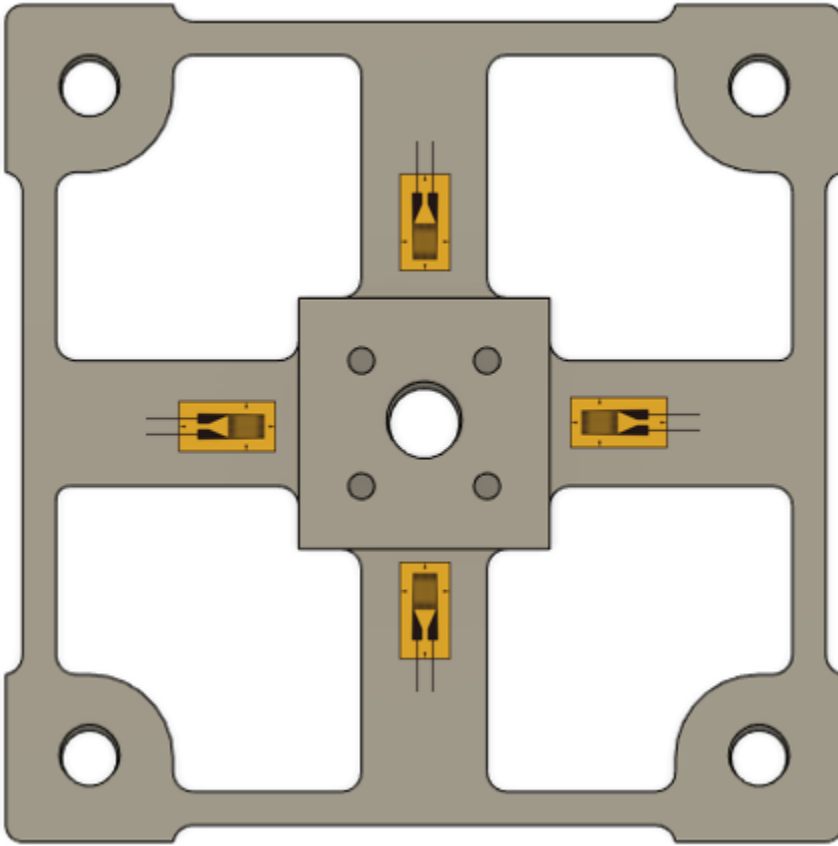


Figure 1: Triaxial loading cell with strain-gauge placement (top)

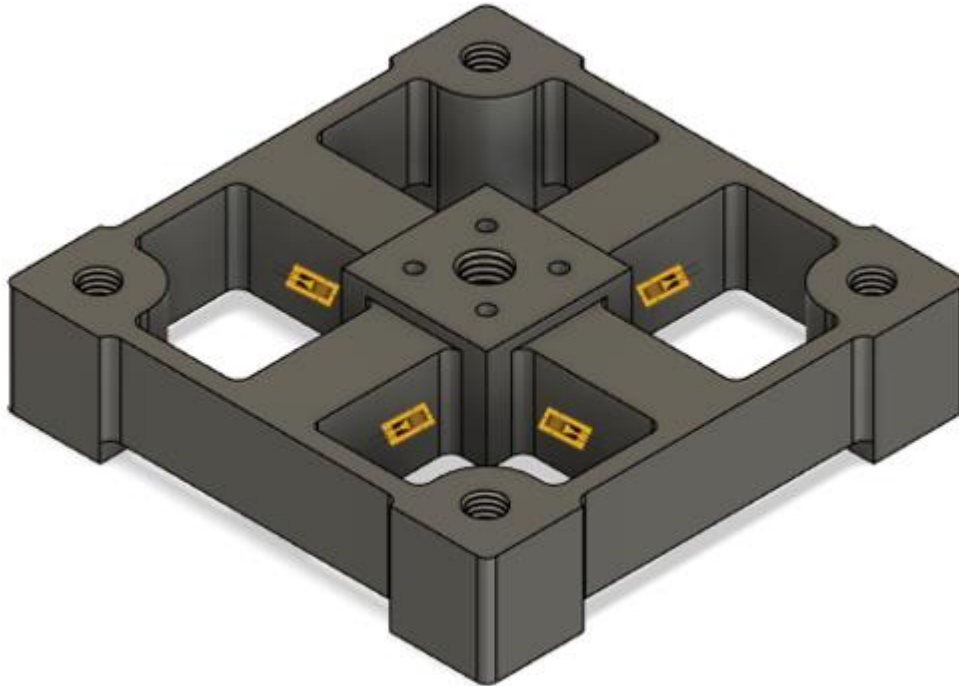


Figure 2: Triaxial loading cell with strain-gauge placement (side)

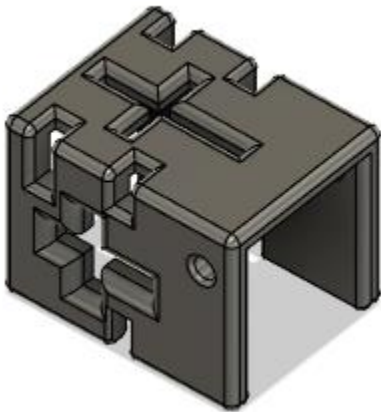


Figure 3: Strain-gauge alignment/marking tool

## CHAPTER 3

### RESULTS

The Z axis was found to have a coefficient of determination ( $R^2$ ) of 0.999 with a theoretical maximum load (corresponding to a 2mv/V standard) of  $\approx 3,800$  N (Figure 4). The Y axis and X were found to have similar  $R^2$  of 0.998 and 0.996 with theoretical maximum loads of  $\approx 2,000$  N. A physical to scaled electrical error of  $\pm 7$  N of force was observed for the Z axis, and  $\pm 5$  N were observed for the X and Y axis, respectively. Maximum mechanical crosstalk between Z and Y/X components was 1.7% or a theoretical full scale 64.6 N of force. This 1.7% falls within the advertised range of  $>2\%$  of the three major force platform manufactures, and well within the limits to be corrected for by a least squares compensation matrix method (Hong et al., 2012)

Table 1: Three-by-three diagonal sensitivity matrix produced for the designed sensor.

	Sensitivity is in microvolts		
	V <sub>fx</sub>	V <sub>fy</sub>	V <sub>fz</sub>
F <sub>x</sub>	3.53	-0.03	0.01
F <sub>y</sub>	0.02	3.51	0.00
F <sub>z</sub>	-0.08	0.06	1.97

Table 2: Measurement error and crosstalk reading of the sensor

Measurement Error and Crosstalk Reading (%)		Axis of Reading	
		Y	Z
Applied Load	Y	-	0.5
	Z	1.7	-

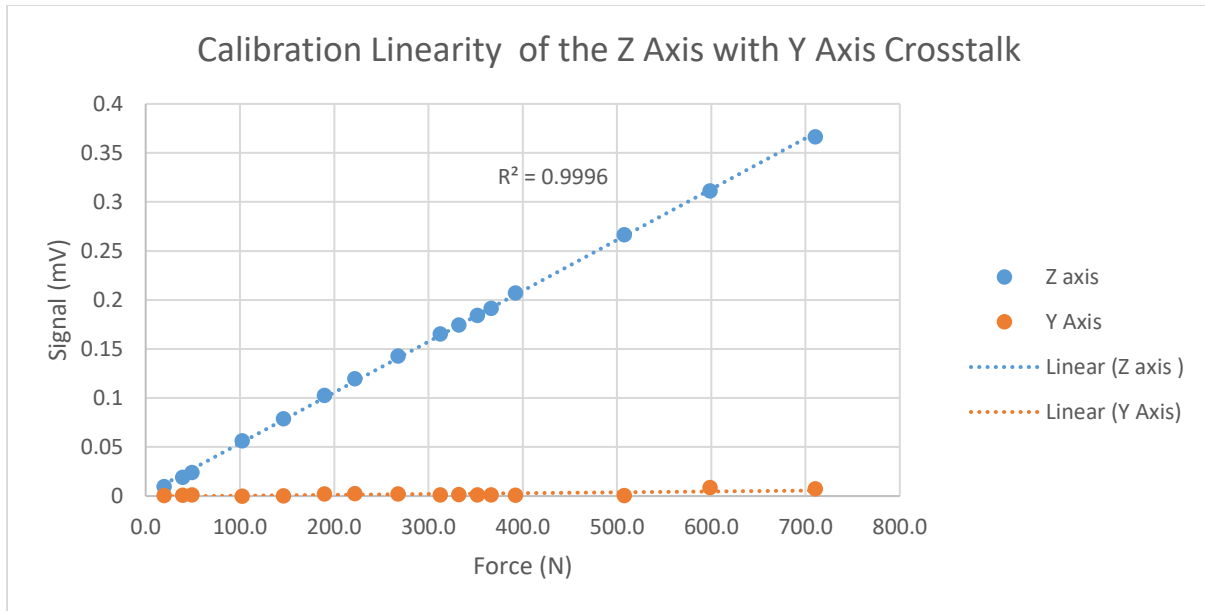


Figure 4: Calibration Linearity of the Z Axis with Y Axis Crosstalk

## CHAPTER 4

### DISCUSSION

The object of this project was to determine the validity and reliability of a custom triaxial force sensor for use in the development of custom force plates to aid scientific research and assess athletic development. Overall, the triaxial force sensor showed adequate resolution with designated applied loads despite the rigidity. This project found high linearity between the applied load and independent component measurements. Resulting in valid and reliable measurements of the vertical force (Z-axis), anterior-posterior force (Y-axis), and mediolateral force (X-axis) magnitudes. Additionally, minimal crosstalk was observed between the vertical component and perpendicular adjacent shear components, with vertical force affecting the perpendicular components by approximately  $>1.7\%$ , and shear components influencing the vertical component by approximately  $>0.5\%$ .

In accordance with Heglund's 8 characteristics of an ideal force-plate, five were directly assessed in this study. To achieve the first two characteristics, the sensor was found to independently resolve the 3 force components, as well as minimize component crosstalk. Sensor linear response, characteristic four, can be termed adequate with an observed coefficient of determination no less than 0.996. Characteristic three states the force sensor needs adequate sensitivity for the question of interest. Keller et. al, 1996 found that an individual running at 6 m/s produces three times their body weight or approximately 2,300N of vertical force. This is well within the projected 3800N capability of the triaxial force sensor, thus achieving the characteristic. The final characteristic requires simplicity and affordable materials, achievement of thus requirements were met with a singular aluminum apparatus with a total cost of  $>500\text{\$}$  US.



Meeting all 5 characteristics with the alignment of a 4 triaxial FP design, the triaxial force sensor can accurately aid scientific research and assess athletic development.

## REFERENCES

- Baena-Raya, A., Soriano-Maldonado, A., Rodríguez-Pérez, M. A., García-De-Alcaraz, A., Ortega-Becerra, M., Jiménez-Reyes, P., & García-Ramos, A. (2021). The force-velocity profile as determinant of spike and serve ball speed in top-level male volleyball players. *PLoS ONE*, *16*(4 April), 1–12. <https://doi.org/10.1371/journal.pone.0249612>
- Baker, D., Wilson, G., & Carlyon, R. (1994). Periodization: The effect on strength of manipulating volume and intensity. *Journal of Strength and Conditioning Research*, *8*(4), 235–242. <https://doi.org/10.1519/00124278-199411000-00006>
- Bates, N. A., Ford, K. R., Myer, G. D., & Hewett, T. E. (2013). Impact differences in ground reaction force and center of mass between the first and second landing phases of a drop vertical jump and their implications for injury risk assessment. *Journal of Biomechanics*, *46*(7), 1237–1241. <https://doi.org/10.1016/j.jbiomech.2013.02.024>
- Bruening, D. A., & Takahashi, K. Z. (2018). Partitioning ground reaction forces for multi-segment foot joint kinetics. *Gait and Posture*, *62*(February 2018), 111–116. <https://doi.org/10.1016/j.gaitpost.2018.03.001>
- Conceição, F., Lewis, M., Lopes, H., & Fonseca, E. M. M. (2022). An evaluation of the accuracy and precision of jump height measurements using different technologies and analytical methods. *Applied Sciences (Switzerland)*, *12*(1). <https://doi.org/10.3390/app12010511>
- Cormie, P., McGuigan, M. R., & Newton, R. U. (2010). Influence of strength on magnitude and mechanisms of adaptation to power training. *Medicine and Science in Sports and Exercise*, *42*(8), 1566–1581. <https://doi.org/10.1249/MSS.0b013e3181cf818d>
- Heglund, N. C. (1981). Short communication: A simple design for a force-plate to measure ground reaction forces. *Journal of Experimental Biology*, *93*(1), 333–338.

<https://doi.org/10.1242/jeb.93.1.333>

Hong, D., Li, C., Jeong, J., 2012. A crosstalk compensation of a multi-axis force/torque sensor based on the least squares method using LabVIEW. Proc. - 4th Int. Conf. Comput. Inf. Sci. ICCIS 2012 1127–1130. <https://doi.org/10.1109/ICCIS.2012.12>

Kebede, G. A., Ahmad, A. R., Lee, S. C., & Lin, C. Y. (2019). Decoupled six-axis force–moment sensor with a novel strain gauge arrangement and error reduction techniques. *Sensors (Switzerland)*, *19*(13), 5–9. <https://doi.org/10.3390/s19133012>

Keller, T. S., Weisberger, A. M., Ray, J. L., Hasan, S. S., Shiavi, R. G., & Spengler, D. M. (1996). Relationship between vertical ground reaction force and speed during walking, slow jogging, and running. *Clinical biomechanics*, *11*(5), 253-259.

Lin, C. Y., Ahmad, A. R., & Kebede, G. A. (2020). Novel mechanically fully decoupled six-axis force-moment sensor. *Sensors (Switzerland)*, *20*(2), 1–19. <https://doi.org/10.3390/s20020395>

Naves, E. L. M., Pereira, A. A., Andrade, A. O., & Soares, A. B. (2009). Design and evaluation of a biomechanical system for athletes performance analysis. *Measurement: Journal of the International Measurement Confederation*, *42*(3), 449–455. <https://doi.org/10.1016/j.measurement.2008.08.010>

Weyand, P. G., Sternlight, D. B., Bellizzi, M. J., & Wright, S. (2000). Faster top running speeds are achieved with greater ground forces not more rapid leg movements. *Journal of Applied Physiology*. <https://doi.org/10.1152/jappl.2000.89.5.1991>

**VITA**

Graduate School  
Southern Illinois University

Kailey A. Reynolds

k.ann.reynolds@gmail.com

University of Wisconsin-Whitewater  
Bachelor of Science, Kinesiology, May 2020

Research Paper Title:

Triaxial Force Sensor Configuration of an In-Ground Force Platform

Major Professor: Sean Quisenberry